EPJ Web of Conferences **37**, 01011 (2012)
DOI: 10.1051/epjconf/20123701011

DIRAC experiment at CERN

Angela Benelli[a] on behalf of the DIRAC Collaboration

JINR Dubna, Zurich University

Abstract. The precise measurements of $\pi^+\pi^-$ and πK atom lifetime allow to check the predictions of Chiral Perturbation Theory for the pion-pion s-wave scattering lengths with isospin 0 and 2 and for the pion-kaon scattering lengths with isospin 1/2 and 3/2. The DIRAC experiment with the latest results is presented together with the proposal for future investigations.

1 Introduction

Pionium ($A_{2\pi}$) is the $\pi^+\pi^-$ hydrogen-like atom, with 378 fm Bohr radius, which decays predominantly into $\pi^0\pi^0$ [1]. The alternative $\gamma\gamma$ decay accounts for only $\sim 0.4\%$ of the total rate [1,2]. Its ground-state lifetime is governed by the $\pi\pi$ S-wave scattering lengths a_I, with isospin $I = 0, 2$.

$$\Gamma_{2\pi^0} \propto |a_0 - a_2|^2 \tag{1}$$

The values of a_0 and a_2 can be rigorously calculated in Chiral Perturbation Theory (ChPT) [3], predicting $a_0 - a_2 = (0.265 \pm 0.004)$ and the $A_{2\pi}$ lifetime $\tau = (2.9 \pm 0.1) \cdot 10^{-15}$ s [4]. The measurement of $\Gamma_{2\pi^0}$ provides an experimental test of the theory. Moving after the production in the target, the Pionium atoms may either decay into $\pi^0\pi^0$ or evolve by excitation (de–excitation) to different quantum states and finally decay or survive (long-lived states) or break up (be ionized) by the electric field of the target atoms. In the case of breakup, characteristic atomic pairs emerge [5] with a low relative momentum Q in their center of mass ($Q < 3\ MeV/c$), and small opening angle in the laboratory frame (< 3 mrad).

A high–resolution magnetic spectrometer ($\Delta p/p \sim 3 \cdot 10^{-3}$) is used [6] to identify the pairs and measure Q with sufficient precision to detect the pionium signal. This signal lies above a continuum background from free (unbound) Coulomb pairs produced from short lived sources ($\rho, \Delta \ldots$) . Other background sources are non–Coulomb pairs where one or both pions originate from a long–lived source ($\eta, \eta', \Lambda, \ldots$) and accidental coincidences from different proton–nucleus interactions.

2 Dirac setup

The experiment is designed for efficent detection of the $\pi^+\pi^-$ pairs with small Q. This is done by selective triggering and by exploiting the high resolution of the spectrometer. The longitudinal (Q_L) and transverse (Q_T) components of Q, defined with respect to the direction of the total laboratory momentum of the pair, are measured with precisions 0.55 MeV/c and 0.10 MeV/c, respectively.

The upstream part of the channel is mainly in vacuum and the detectors have been designed so to reduce at maximum the effect of the multiple scattering of the particles and preserve the small Q distribution of the pairs. After the target we had, till 2003, 4 planes of GEM-MSGC that have been replaced with Micro Drift Chambers (MDC). Then 3 planes of Scintillator Fibres (SFD) provide a spatial resolution for isolated tracks or close tracks of $\delta_{isolated} = 0.022cm$ and $\delta_{close} = 0.055cm$ respectively [7]. When only one fibre is hit in a plane we use the same orientation plane of Ionisation

[a] e-mail: angela.benelli@cern.ch

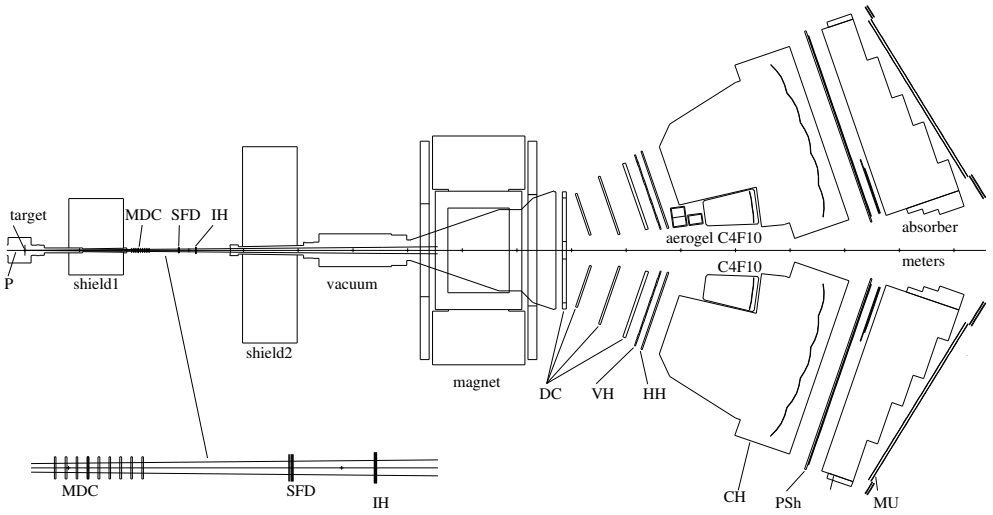

Fig. 1. DIRAC setup: MDC are microdrift gas chambers, SFD is a scintillating fiber detector and IH is a scintillation ionization hodoscope. Downstream the spectrometer magnet there are drift chambers (DC), vertical (VH) and horizontal (HH) scintillation hodoscopes, Cherenkov detectors containing nitrogen (CH), heavy gas C4F10 and aerogel radiators, shower detectors (PSh) and scintillation muon detectors (MU).

Hodoscope (IH) in order to distinguish if the energy deposited corresponds to a single track or a pair crossing the same IH slab. A 1.65 Tesla dipole magnet is used for the momentum determination. After the magnet there are 4 groups of Drift Chambers, consisting of X, Y and W (inclined) planes giving a spatial resolution of $85\mu m$. Then a Vertical Hodoscope (VH) consisting of 20 scintillating slabs with a time resolution below $140ps$ is used for particle timing, and an Horizontal Hodoscope (HH) is used by the trigger in order to select opposite charged particles with a vertical displacement smaller than $75mm$.

The experimental resolutions on the momentum and opening angle must be accurately simulated in order to extract the narrow pionium signal. Multiple–scattering in the target is the primary source of uncertainty on the Q_T measurement. In order to achieve the desired Q_T resolution, the scattering angle in the target must be known with $\sim 1\%$ precision.

Using this configuration of the DIRAC detector we have published our last analysis of $\sim 1.5 \cdot 10^9$ events grouping the data from 2001 till 2003 [8]. These data come from collisions of 20 and 24 GeV/c protons, delivered by the CERN PS, impinging on a thin Ni target foil of 94 or 98 μm thickness for different run periods.

In Figs. 2, the $|Q_L|$ and Q_T projections of the experimental prompt $\pi^+\pi^-$ spectrum are shown in comparison to the fitted simulated background spectrum. After subtraction of the background, the experimental $A_{2\pi}$ signal emerges at small values of $|Q_L|$ and can be compared with the simulated signal. The overall agreement between the best–fit experimental and simulated spectra is excellent, over the entire Q_T, Q_L domain. We have detected $n_A = 21227 \pm 407$ atomic pairs, that allow us to give our final measurement of the ground–state $A_{2\pi}$ lifetime yielding

$$\tau = [3.15^{+0.20}_{-0.19}(\text{stat})^{+0.20}_{-0.18}(\text{sys})] \cdot 10^{-15} \text{ s}.$$

We obtain the $\pi\pi$ scattering length difference

$$|a_0 - a_2| = [0.2533^{+0.0078}_{-0.0080}(\text{stat})^{+0.0072}_{-0.0077}(\text{sys})]M^{-1}_{\pi^+}.$$

Our result is compatible with the theoretical prediction and with the other experiment, NA48, that provides a measurement of $a_0 - a_2$, [9].

In 2007 we have modified the DIRAC setup in order to study the $K\pi$ atomic pairs at the same time as collecting more statistics for $\pi\pi$ atomic pairs. In both arms the Nitrogen Cerenkov detectors (N_2)

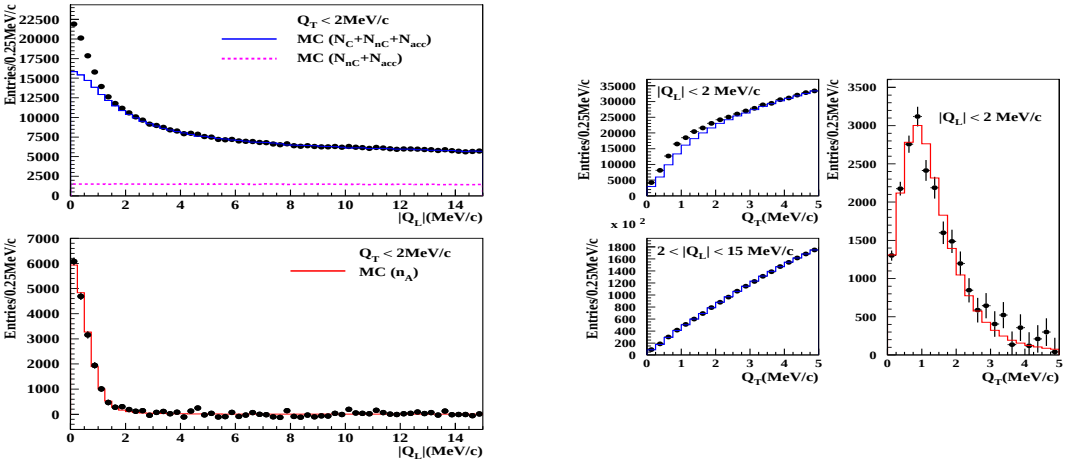

Fig. 2. On the right : $|Q_L|$ fit projections of the $\pi^+\pi^-$ spectrum from data (dots) and simulation (full line). The top plot shows the simulated background components compared with the experimental spectrum; the bottom plot shows the pionium signal after background subtraction and the simulation. On the left: Q_T fit projections of the $\pi^+\pi^-$ spectrum from data (dots) and simulation (full line). Top left: in the $A_{2\pi}$ signal region; bottom left: away from the signal region. Right: pionium signal after background subtraction and simulation.

have been cut to have the space to install the heavy gas C_4F_{10} Cerenkov detectors. With an efficiency of more that 99% they identify pions while not responding to kaons or (anti)protons. The average number of photoelectrons is 28 for particles with $\beta = 1$. Next to the N_2 only on the left side, we have installed an Aerogel Cerenkov detector that identify kaons and reject protons. The detector consists of three modules, the two in front have a refractive index of 1.015, typically 10 photoelectrons for a particle with $\beta = 1$. Their efficiency is better than 98% for kaons with momentum below $5.5 GeV/c$ with only 11% contamination of protons. The module in the back has a refractive index of 1.008 and covers the higher momentum range of the kaons, between $5.5 - 8 Gev/c$, the average number of photoelectrons is $4 - 5$ for a $\beta = 1$ particle.

The preshower detector (PSh) provide an additional electron/hadron separation to the N_2 Cerenkov, and his performance has been increasingly important after the cutting of the Ni Cerenkov in order to keep the level of electron rejection at the level of 98% [10]. With this modified detector and using only the downstream part of DIRAC for the tracking we have published the result of the $K\pi$ analysis [11].

We have detected an excess of low Q events with a significance of 3.2σ, $n_A^{K\pi} = 173 \pm 54$. If these events are interpreted as atomic pairs, then we can estimate a lower limit on the mean lifetime for $K\pi$ atoms of $0.8 fs$ with a confidence level of 90%.

The data collected in 2008-9-10 shown in Figure 3 have been analysed and the preliminary results are with a significance of 5.3 sigma, this will provide a value for $|a_{1/2} - a_{3/2}|$ with a relative error of 26%.

3 Long-lived Atoms

In order to get the values of the a_0 and a_2 scattering lengths separately from $\pi^+\pi^-$ atoms data, one may exploit the fact that the energy splitting between the levels ns and np, $\Delta E_n = E_{ns} - E_{np}$, depends on an other combination of the scattering lengths: $2a_0 + a_2$ [12]. The energy splitting for the levels with the principal quantum number n and orbital quantum number l includes few contributions:

$$\Delta E_{nl} = \Delta E_{nl}^{em} + \Delta E_{nl}^{vac} + \Delta E_{nl}^{str} \tag{2}$$

where ΔE_{nl}^{em} includes relativistic insertions, finite-size effect, self-energy corrections due to transverse photons and transverse photon exchange. The term ΔE_{nl}^{vac} includes the contributions from the vacuum

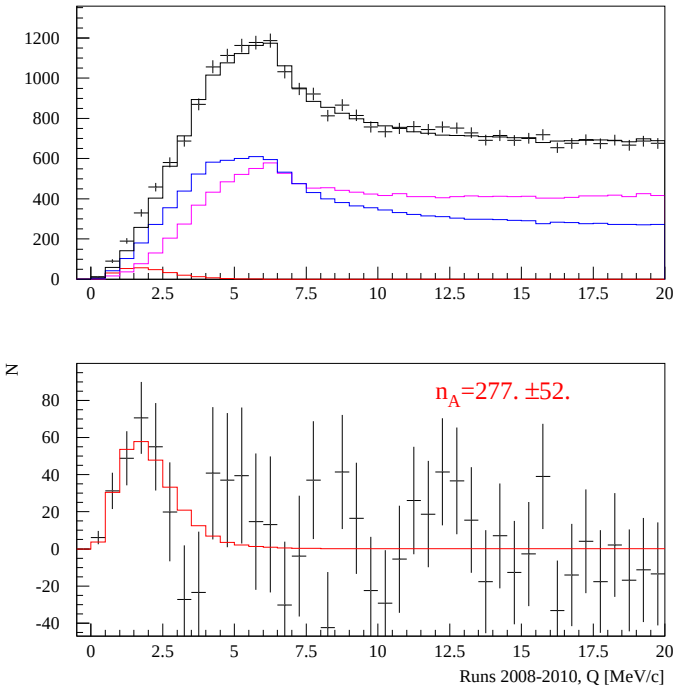

Fig. 3. The top plot shows the simulated background components compared with the experimental spectrum (points with errors), in blu the Coulomb pairs, in magenta the non-Coulomb, in red the atomic pairs; the bottom plot shows the residuals between data and the fitted background for $\pi^- K^+$ and $\pi^+ K^-$ for the 2008-2009-2010 data.

polarization. The last term ΔE_{nl}^{str} takes into account strong interaction effects and it's related to the $\pi\pi$ scattering lengths as follows: $\Delta E_{nl}^{str} = A_n(2a_0 + a_2)$. The theoretical value for the 2s-2p energy splitting has been calculated as $\Delta E^{2s-2p} = -0.59 \pm 0.01 eV$ [13]. By measuring the value ΔE^{2s-2p} we can determine the numerical value of ΔE_{nl}^{str} substituting the other terms in equation 2 that have been calculated with a high accuracy. The method for measuring ΔE_n was discussed in [14].

In inclusive processes, $A_{2\pi}$ are produced in s-states distributed over the principal quantum number n proportionally to n^{-3}. When moving inside the target, the relativistic $A_{2\pi}$ interacts with the target atoms and, with some probability (depending on the material), will leave the target with orbital angular momentum $l > 0$.The main part of these atoms will be in the 2p-state. For $A_{2\pi}$ in np-state the decay into two π^0 mesons is forbidden by the conservation law for the angular momentum, and the process $A_{2\pi} \rightarrow \pi^0 + \gamma$ is also strongly suppressed. Therefore, the main mechanism of the np-states decay is the np $\rightarrow$ 1s radiative transition with a subsequent annihilation from the 1s-state into two π^0 with a lifetime of $\tau_{1s} \sim 3 \times 10^{-15} s$. The lifetime of the atom in the 2p-state is determined by the radiative transition probability equivalent to $\tau_{2p} = 1.17 \times 10^{-11} s$. This is why we refer to them as "long lived", 3 order of magnitude slower decay time compared to the s-state $A_{2\pi}$. For the average $A_{2\pi}$ momentum in DIRAC of $4.5 GeV/c$ the corresponding decay length is 5.7 cm for 2p-state, 19 cm for 3p and bigger for the increasing p.

The influence of a constant magnetic field on the $A_{2\pi}$ atom lifetime has been studied. The transverse magnetic lab. field B_0 is increased to $B = \gamma B_0$ in amplitude in the atom reference frame. The corresponding electric field is perpendicular to the atom momentum, and it will allow the admixture of the ns-state with the np-state wave functions. This admixture may cause a significant faster decay for atoms initially being in the np-state. For the case of $B_0 = 4T$ and $\gamma = 20$, the decay rate increases more than twice for the 2p state.

4 Search for Long-lived atoms

As a first step, during the 2011 and 2012 data taking DIRAC had as objective the observation of long lived atoms. In order to do so, after the Be target installed as the primary target, we have installed at 10 cm distance a Platinum foil ($d = 2\mu m$), [15].

The proton interaction with the Be target ($d = 100\mu m$) produces $A_{2\pi}$ that can decay or break in $\pi^+\pi^-$ pairs, Coulomb pairs and non-Coulomb pairs. Around 6% of $A_{2\pi}$ will leave the target in a np-state, thus they will not have the time to decay before reaching the Platinum foil, where they will break into $\pi^+\pi^-$ pairs. We will be able to detect in DIRAC the $\pi\pi$ atomic-pairs created in the Pt foil above the background formed by the $\pi^+\pi^-$ pairs created in the Be target.

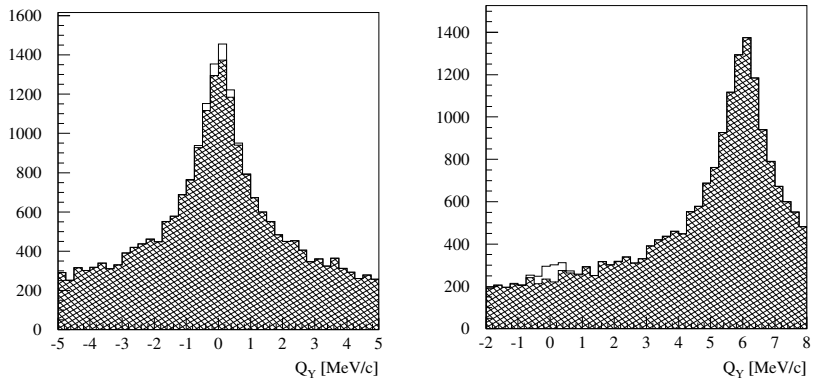

Fig. 4. Q_Y distribution of pairs without and with the magnet.

To reduce strongly this background a magnet has been installed between the Be target station and the Pt foil: the $0.01Tm$ magnet shifts the Y component of the relative momentum Q. In figure 4 it's shown the Q_Y distribution with and without the magnet, in black is the simulation result for the Q_Y of the pairs produced at the Beryllium target,(on the right is centered at $6MeV/c$) in white the Q_Y distribution of the pairs produced at the Pt foil (with the magnet on, centered in $Q_Y = 0$).

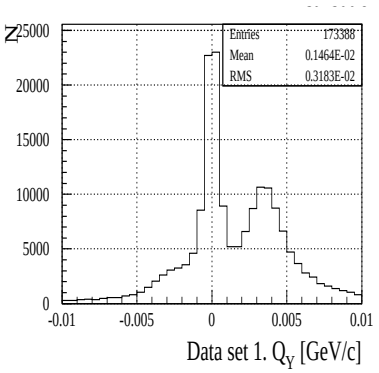

Fig. 5. e+ e- data 2010, Q_Y distribution of pairs generated at the Be-target are shifted on the right $Q_y > 0$, while the pairs generated at the Pl-foil are centered in $Q_Y = 0$.

The electron-positron data taken during 2011 confirms the results of the simulation. In order to have a bigger Q_Y shift we have installed this year (2012 data) a new stronger magnet, Sm_2Co_{17}, high resistivity against radiation. This will allow us to extract a signal with a significance of more than 9 sigma.

For the future, DIRAC plans to move to the SPS accelerator. With the proton energy of 450 GeV/c, the yield of $A_{2\pi}$ and $A_{\pi K}$ will increase of a factor 20 per proton-nucleus interaction.

References

1. J. Uretsky and J. Palfrey, Phys. Rev. **121** (1961) 1798
2. J. Gasser *et al.*, Phys. Rep. **456** (2008) 167
3. S. Weinberg, Physica **A96** (1979) 327; J. Gasser and H. Leutwyler, Phys. Lett. B **125** (1983) 325; *ibid* Nucl. Phys. B **250** (1985) 465, 517, 539
4. G. Colangelo *et al.*, Nucl. Phys. B **603** (2001) 125
5. L.L. Nemenov, Yas Fiz **41** (1985) 980; Sov. J. Nucl. **41** (1985) 629
6. B. Adeva *et al.*, Nucl. Instrum. and Meth. A **515** (2003) 467
7. *SFD study and simulation for the data 2008-2010*, A. Benelli [Zurich], DIRAC-TALK-2011-01
8. B. Adeva *et al.*, Physics Letters B **704** (2011) 24
9. J.R. Batley *et al.*, Eur. Phys. J. C **64** (2009) 589; J.R. Batley *et al.*, Eur. Phys. J. C **70** (2010) 635
10. M. Pentia, S. Constantinescu, M. Gugiu [IFIN-HH], DIRAC-NOTE-2011-03
11. B. Adeva *et al.*, Physics Letters B **674** (2009) 11
12. S. Deser *et al.*, Phys Rev **96** (1954) 774 and G.V. Efimov, M.A.Ivanov and E.E. Lyubovitskij, Yad. Fiz. **44** (1986) 460; Sov. J. Nucl. Phys. **44** (1986) 296
13. J. Schweizer, Phys. Lett. B **587** (2004) 33
    J. Schweizer, Eur. Phys. J. C **36** (2004) 483
14. L. L. Nemenov and V. D. Ovsyannikov, Phys. Lett. B **514** (2001) 247; L. L. Nemenov, V. D. Ovsyannikov and E. V. Chaplygin, Nucl. Phys. A **710** (2002) 303
15. DIRAC-DOC-2012-01: PS212 Addendum 6, CERN-SPSC-2012-001 (SPSC-P-284-ADD-6).